High-Precise Fractional Orbital Angular Momentum Probing with a Fiber Grating Tip

Guoxuan Zhu, Zhao liu, Cailin Fu, Shen Liu, Zhiyong Bai, and Yiping, Wang, Senior Member, IEEE, Senior Member, OSA

***Abstract*—Optical orbital angular momentum (OAM), carried by optical vortices, is a fundamental property of light that grabs broad interests. The detection of OAM modes, including fractional OAM is of great importance in diverse fields. Here, we firstly propose and develop the limited integer-component measurement method to determine the fractional topological charge (TC) of OAM states. This method indicates that a 2-integer-mode responsive device could be applied for the detection of fractional TC. An orthogonal long-period fiber grating (OLPFG) element is used as a fractional OAM TC probe to verify the Applicability. We experimentally demonstrate the fractional TC detection, ranging from -1 to 0, and recognize different fractional OAM modes with the minimum TC interval of 0.01. This scheme provides a concise, precise, continuous, and fiber-compatible fractional TC detection method that might have great potential in micro-detection, optical communication, quantum information and chiral sensing applications.**

***Index Terms*—fractional orbital angular momentum, fiber sensor, long period fiber grating**

I. Introduction

Orbital angular momentum (OAM) modes have gained huge interests and demonstrated great success in diverse fields since it was first recognized in 1992 [1]. The helical phase structure, expressed as $\exp(il\varphi)$, where l is the topological charge (TC) of the OAM, gives OAM modes twisting characteristics [2]. When the value of l takes non-integer, the optical vortex beam is named as fractional OAM mode. The fractional OAM modes can be regarded as the superposition of infinite integer OAM modes [3]. Fractional OAM modes present unique properties such as the phase discontinuity [4], perfect vortex defects [5] and Hilbert's hotel paradox [6]. Recently, OAM modes have been proved great potential in the applications of classic communication [7], quantum information [8], particle manipulation [9], optical processing [10], diffraction limit overcoming [11] and spin detection [12]. Therefore, it is of great significance to develop a precise and concise TC detection method.

The detection of OAM TC can be roughly divided into four categories. (a) Bulk optical elements based vortex phase demodulation, e.g. spatial light modulator (SLM) and Dove lens [13-15]. (b) Micron-structured integrated devices such as 3-D waveguides [16], micron rings [17,18] and metasurfaces [19]. (c) Beam pattern recognition, assisted by slits, tilt lens or computer algorithms [20-23]. (d) The OAM mode sorter based on transformation optics [24-26]. Due to the asymmetric intensity distribution effected by non-integer phase singularity, the distinguishing of fractional TC faces more difficulties than the integer TC, both in the accuracy and resolution. Recently, Deng et al. have proposed a precise fractional OAM detection method using a 2D multifocal array [15]. The idea is to decompose the fractional OAM state into adequate number of integer OAM components for fractional TC retrieving. The energy of each integer OAM component is detected by a 2D multifocal array. We find this method can be further improved that only two integer components are minimally needed for precise fractional TC determining. This indicates a system with different response to more than two integer OAM modes can be employed for fractional TC probing. Optical fiber is an important medium for OAM mode transmitting and modulation. However, the fiber OAM modes are strongly coupled due to the pervasive perturbation along the optical fiber [27]. Writing chiral gratings in a few-mode fiber can decouple the degenerate OAM TCs [28,29]. Through the modification of chiral gratings, a fiber device can be employed as a fractional TC micro-probe.

In this letter, we proposed the theory of limited integer-component measurement method that the fractional TC of an OAM mode can be determined via testing the energy of its arbitrary two integer components. The feasibility of this method is verified by a free-space Dammann grating experiment. The error of the fractional TC detecting result is less than 0.035 (determined by the response accuracy of our InGaAs camera). Based on this principle, an OLPFG (reported in [30] for generating pure OAM modes) is applied to measure the fractional OAM TC. The variety spectral responds to 0 and ±1 modes of OLPFG are firstly explored. The fractional OAM TC of the input beam is determined according to the spectral

Manuscript revised XXX; accepted XXX. Date of publication XXX; date of current version XXX. This work was supported in part by the National Natural Science Foundation of China (NSFC) (62005169, 61875134, 61635007); Natural Science Foundation of Guangdong Province (2019A050510047, 2019B1515120042); Science and Technology Innovation Commission of Shenzhen (JCYJ20180507182058432, JCYJ20180507182035270) (Corresponding author: Zhiyong Bai.)

The authors are with 1. Key Laboratory of Optoelectronic Devices and Systems of Ministry of Education/Guangdong Province, College of Physics and Optoelectronic Engineering, Shenzhen University, Shenzhen 518060, China. 2. Shenzhen Key Laboratory of Photonics Devices and Sensing Systems for Internet of Things, Guangdong and Hong Kong Joint Research Centre for Optical Fiber Sensors, Shenzhen University, Shenzhen 518060, China. (e-mail:, zhugxuan@szu.edu.cn; 1810285080@email.szu.edu.cn; fucailing@szu.edu.cn; shenliu@szu.edu.cn; baizhiyong@szu.edu.cn; ypwang@szu.edu.cn).

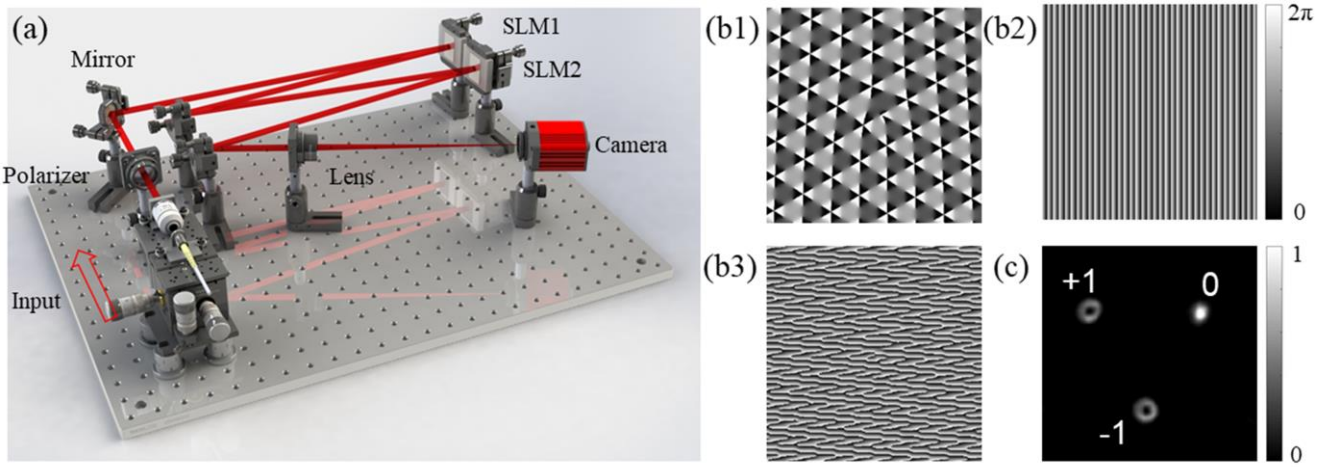

Fig. 1. (a) Diagram of free-space experiment setup. (b1) The Dammann grating consists of +1, 0, -1 integer orders. (b2) Linear grating to eliminate the zero order diffractive light. (b3) The hologram pattern loaded on SLM2 to demultiplex three integer OAM components. (c) The demultiplex result of incident Gauss beam.

shape analysis. Furthermore, an SLM is used to generate arbitrary fractional input modes ranging from l=-1 to l=0 for experiment demonstration. The resolution of the TC recognition reaches to 0.01, which is comparable to the state-of-art result shown in [21] supported by the deep learning algorithm.

II. Method

A general fractional OAM mode might contain sophisticated integer OAM components according to diverse generation methods [31-33]. Here, we only focus on the restricted fractional OAM modes with a single fractional TC. The transverse complex field of the fractional OAM modes can be described by

$$E_m = F_m(r)\exp(im\varphi + i\varphi_0) \tag{1}$$

Where $F_m(r)$ is the radial field distribution, m is the fractional TC, φ is the transverse angle, and φ_0 is the initial phase. Equation (1) can be decomposed into the base of integer OAM states by Fourier transformation as

$$E_m = \sum_{l=\infty}^{\infty} A_m^l \exp(il\varphi) \tag{2}$$

Where A_m^l is the l^{th} integer Fourier coefficient and expressed as

$$A_m^l = \frac{\exp(im\pi)\sin(m\pi)}{\pi(m-l)}\int F_m(r)e^{i\varphi_0}\,2rdr \tag{3}$$

According to (3), the ratio of p^{th} and q^{th} integer OAM weights can be calculated by a simple expression

$$\left(\frac{A_m^p}{A_m^q}\right)^2 = \left(\frac{m-q}{m-p}\right)^2 \tag{4}$$

Equation (4) is divided into three situations, $m<p$; $p<m<q$ and $q<m$. In each case, the value of m can be continuously determined by measuring the value of the ratio of p^{th} and q^{th} integer OAM components. The measurement accuracy is dependent on the detection accuracy of p^{th} and q^{th} integer OAM components of the input fractional OAM. In order to illustrate the principle of the method, we experimentally use a free-space Dammann grating for demonstration.

A. Free-space fractional OAM detecting

The setup of the experiment is shown in Fig. 1(a). A 1550 nm light source is ejected from the fiber end of a tunable laser and collimated into free-space. Then the light passes through a linear polarizer. The spatial light modulator 1 (SLM1) is employed to generate fractional OAM. Meanwhile, the SLM2 uploads the Dammann grating, shown in Fig.1(b3), to demultiplex the incident beam into three integer components, l=-1, 0 and +1. Fig. 1(b1) is a pure Dammann grating to separate the three integer components. The separating angle sets $2/3\cdot\pi$ to avoid the effect of high order diffraction points. Fig. 1(b2) is a linear grating to move the resulting pattern away from the zero order diffraction point. The pattern in Fig. 1(b3)

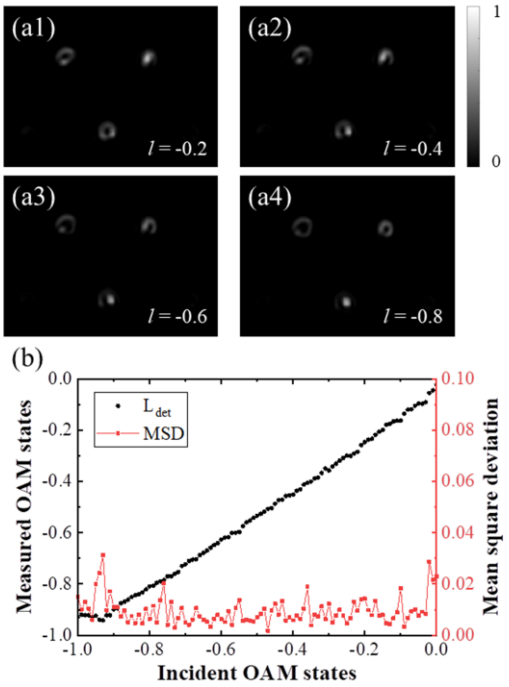

Fig. 2. The demultiplex results of (a1) l=-0.2, (a2) l=-0.4, (a3) l=-0.6, and (a4) l=-0.8

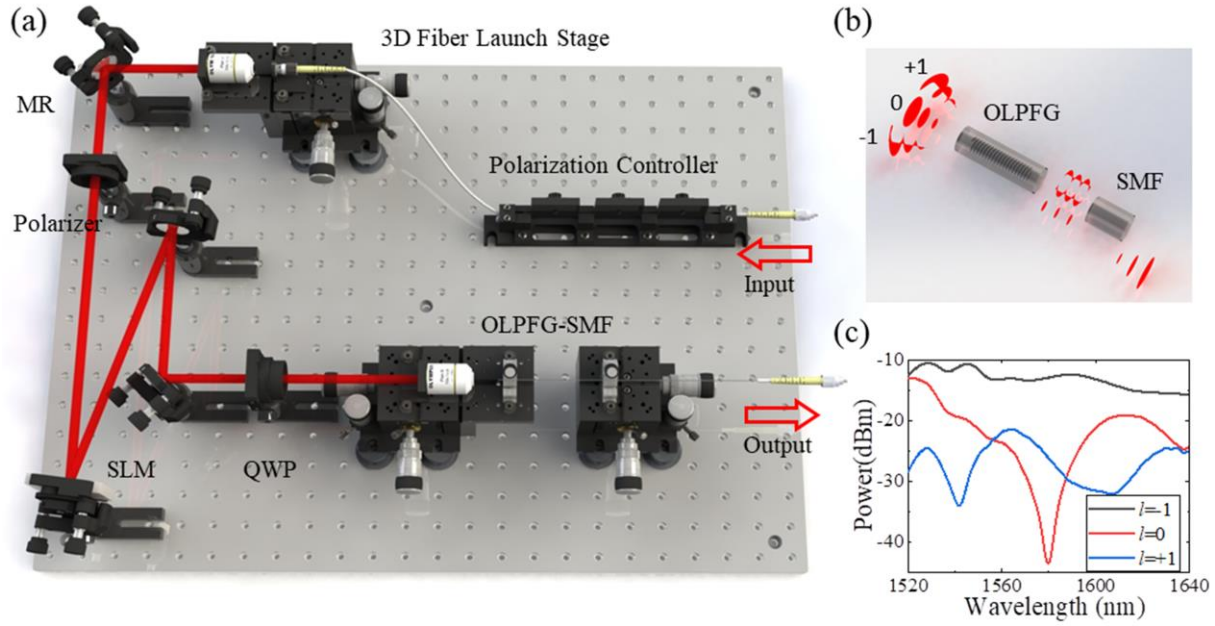

Fig. 3. (a) Experiment setup for fractional OAM mode probing. A narrow-band tunable laser is used for alignment and an ASE source is used as input for spectral measurement. The output port connects to the OSA. (b) Sketch of the OLPFG fractional OAM mode probe. (c) Spectral response to OAM modes with -1, 0, and +1 TCs.

is the direct addition of (b1) and (b2). After the Fourier transformation induced by a lens, the pattern of the demultiplexing result is recorded by an InGaAs camera. When the beam illuminating on SLM2 is a Gauss beam, the pattern on camera is shown as Fig.1(c). Each corresponding integer OAM component will be converted into a Gauss-like spot at the pre-set position on the camera plane, the up-left spot for l=+1, up-right for l=0 and down-middle for l=-1.

An arbitrary fractional TC could be decomposed into an integer (l_I) part and a fractional (l_F) part. The integer part only affects the entire shift of the vortex spectrum of the beam. The detection of a high order fractional TC can be simplified into the detection of the fractional part, $-1<l_F<0$, by adding a conjugate integer ($-l_I$) vortex phase on the hologram shown as Fig. 1 (b3). Therefore, the main interest of Fourier coefficients evolution is then focused on the fractional part that $-1<l_F<0$ [15]. In the experiment, the TCs range from l=-1 to l=0 with the interval of 0.01 are chosen for testing. The demultiplex pattern of each fractional TC is captured 8 times. Some of the recorded patterns are extracted as shown in Fig. 2(a1)-(a4). We use the spots of l=0 and -1 to calculate the fractional TC charge, while spot of l=+1 to check that the incident fractional TC is between l=-1 and 0 (the energy of Gauss-like spot l=+1 is less than l=-1 or 0). In order to get a high signal-noise ratio, only the central 4 pixels of each preset position are taken into calculation. Equation (4) could be rewritten with q=0 and p=-1as

$$m = \frac{-\sqrt{I_m^{-1}}}{\sqrt{I_m^{0}} + \sqrt{I_m^{-1}}} \tag{5}$$

Where I_m^0 and I_m^{-1} are the energy of recorded central pixels of the spots l=0 and -1 separately. The calculated TCs with the experiment data is shown in Fig. 2(b). The measured TCs are almost equal to the incident beam and the mean square deviation is less than 0.035. The flat response from l=-1 to l=-0.9 might be caused by the background noise of the I_m^0 detecting pixels. Due to the good linear response, the measuring accuracy could be further refined with pre-calibration.

B. Fiber grating fractional OAM probing

According to the limited integer-component measurement method, a 2-integer-mode responsive system can be employed for fractional TC probing. Under the guidance of this principle, an OLPFG-SMF device is applied as a fractional TC micro-probe. A fractional OAM beam can be decomposed into the superposition of a number of integer-order OAM beams. Each integer mode features individual dispersion curve when passing through the grating, as illustrated in Fig. 3(c). With fine chiral structure design, the OLPFG has different spectral response to l=0, -1 and +1 integer OAM modes while a common LPFG cannot recognize the difference between ±1 OAM modes [30]. As a result, the weight of the integer-order components can be retrieved by analyzing the spectrum response. It is worth noting that the fiber grating will have the best spectral performance because of the lowest insertion loss, when m takes a fractional number between -1 and 0.

The experimental setup is shown in Fig. 3(a). The input light source passes through a polarization controller and launches into free space by a 3D motion stage. A narrow-band tunable laser is used for the optical path alignment while a wide-band amplified spontaneous emission (ASE) source is used for the spectral measurement. A polarizer and an SLM are used to load a fractional vortex phase on the free-space Gauss beam. Then the modulated beam is converted to the left-hand circular-polarized state by a quarter-wave plate (QWP). The OLPFG is written on a two-mode fiber to collect the fractional OAM beam. By carefully adjusting the two mirrors set before the QWP, the generated fractional OAM beam is finely aligned to the fiber end. A 3m-length SMF is spliced to the OLPFG as a mode filter. The output SMF pigtail is connected to an OSA for

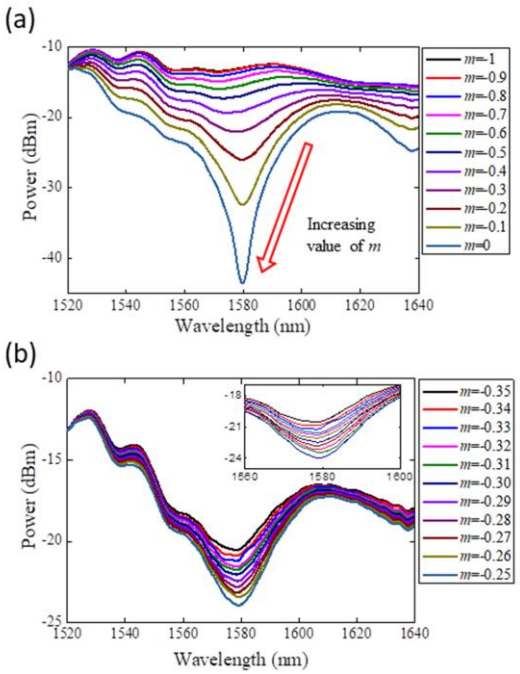

Fig. 4. Spectral responses to fractional OAM modes (a) with TCs range from -1 to 0, (b) refined adjacent modes with 0.01 steps from -0.35 to -0.25.

spectral measurement.

III. Result

The fractional TC probe is consisting of an OLPFG and an SMF pigtail. The working principle is shown in Fig. 3(b). The period of LPFG is 960 μm, which determines that the coupling occurs between the 1st order and the fundamental mode groups. Meanwhile, the orthogonal grating is designed to be chirality selective and induces the coupling occurs between l=0 and -1. As a result, through the OLPFG, l=-1 mode is converted to fundamental mode (l=0), fundamental mode is converted to l=-1, and l=+1 keeps insulation. After the SMF mode filter, only the fundamental mode can pass through. Noting that, a common LPFG cannot recognize the chirality of the input mode, due to strong coupling between l=±1. Therefore, launching ±1 modes into a common LPFG, one can only receive identical spectrum after the SMF pigtail. Fig. 3(c) shows the spectral response of -1, 0, and +1 OAM modes. Due to the applying of free-space coupling, the optical path has large insertion loss close to 10 dB, including around 5 dB lens loss, 2 dB polarization plate loss, 1 dB SLM diffraction loss, and around 2 dB coupling loss. The -1 order OAM mode can pass through the probe, and presents a relatively flat response spectrum. The coupling between the fundamental and -1 order modes are well optimized during the fabrication process. So that the highest conversion efficiency is close to 99.9% (-30dB extinction ratio). Due to the influence of orthogonal gratings, the input +1 mode can barely convert to fundamental mode, and the conversion efficiency is less than 10% (<-10dB). Therefore, the probe shows a good performance that -1, 0, and +1 OAM modes have varied spectral response. When inputting a fractional OAM mode, the response spectrum can be regarded as the superposition of the separating integer OAM spectrum. The depth of the dip on the spectrum reflects the proportion of 0 and

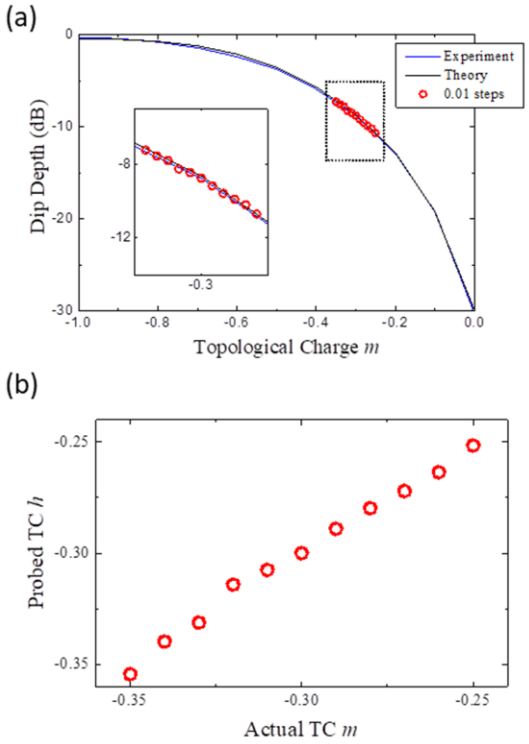

Fig. 5. The recognition of response spectrum. (a) Dip depth versus input TCs, (b) The probed TCs.

-1 OAM components. According to (4), the dip depth of the m^{th} OAM mode can be determined by

$$10^{0.1\cdot D_m} = A_{-1}^{m}10^{0.1\cdot D_{-1}} + \alpha\cdot A_{0}^{m}10^{0.1\cdot D_0} + A_{1}^{m}10^{0.1\cdot D_1} \quad (6)$$

Where D_{-1}, D_0, D_1, D_m, are the dip depth of measured -1, 0, 1, and m spectrum respectively, α is the coefficient of the coupling efficiency difference between 0 and 1 mode groups, experimentally takes 1.2. The dip depth of an arbitrary fractional OAM mode (m ranges from -1 to 0) can be theoretically predicted using (6) as shown in Fig. 5(a).

The detected spectrum of the fractional OAM modes on the output side is shown in Fig. 4, including (a) TC range from -1 to 0 with 0.1 steps and (b) from -0.35 to -0.25 with super-high resolution of 0.01 steps. The spectrum ranges from 1520nm to 1640nm, containing 4001 points (0.03nm resolution). All the modes are detected under the left-hand polarization state. As predicted by (4) and (6), each fractional TC corresponds to one dip depth. The depth of the spectrum dip increases with the value of fractional TC m. It worth noting that, besides the dip depth, the shape of the responding spectrum can also be predicted by (6) provided the response spectrums of the integer components are pre-tested. The spectrum shape matches well with the experiment results in Fig.4, even when the TC recognition is as fine as 0.01.

The relationship of the dip depth and m value is shown in Fig. 5(a). The depth of the spectrum is calculated by minus the value of spectrum points at 1580.4nm to the value at 1520nm. In order to eliminate the fluctuation, 20 points around the two wavelengths are taken into calculation. The black line, theoretical result, is calculated using (6) with the integer OAM spectrum data shown in Fig. 3(c). The blue line, experimental

result, is plotted based on the spectrum data shown in Fig. 4(a). These two lines match well along the whole detection region, -1<m<0. The red circles are the measured depth value of the super-high resolution fractional OAM modes shown in Fig. 5(b).

According to the theory relationship between the spectrum depth and TC, as (6), the value of *m* can be probed as shown in Fig. 5(b). The resolution is 0.01 and the error between the probed TC and the real TC is less than 0.006. That indicates a 2-integer-mode responsive device can be employed for concise and precise TC detecting.

IV. Conclusion

To summarize, we have proposed the limited integer-component measurement method for fractional TC detection. The fractional order TC could be determined by detecting the ratio of its two integral order components. A free-space Dammann grating and an OLPFG-SMF micro-probe are applied to verify the effectiveness of this scheme. The good agreement between the theoretical and experimental results indicates that the limited integer-component measurement method has super high accuracy. This method provides a precise, convenient and fiber-compatible scheme for the measurement of fractional TCs that might be used in microstructure detection, fiber communication, and quantum information.

References

[1] L. Allen, M. W. Beijersberge, R. J. C. Spreeuw, and J. P. Woerdman, "Orbital angular momentum of light and the transformation of Laguerre-Gaussian laser modes," Phys. Rev. A vol. 45, no. 11, pp. 8185, 1992.

[2] G. Molina-Terriza, J. P. Torres, & L. Torner, "Twisted photons," Nature phys. Vol. 3, no. 5, pp. 305-310, 2007.

[3] J. Leach, E. Yao, and M. J. Padgett, "Observation of the vortex structure of a non-integer vortex beam," New J. Phys. Vol. 6, no. 71, 2004.

[4] J. B. Götte, K. O'Holleran, D. Preece, F. Flossmann, S. Franke-Arnold, S. M. Barnett, and M. J. Padgett, "Light beams with fractional orbital angular momentum and their vortex structure," Opt. Express vol. 16, no. 2, pp. 993-1006, 2008.

[5] G. Tkachenko, M. Chen, K. Dholakia, and M. Mazilu, "Is it possible to create a perfect fractional vortex beam," Optica vol. 4, no. 3, pp. 330-333. 2017.

[6] G. Gbur, "Fractional vortex Hilbert's hotel," Optica vol. 3, no. 3, pp. 222-225. 2016.

[7] J. Wang, J. Y. Yang, I. M. Fazal, N. Ahmed, Y. Yan, H. Huang, Y. Ren, Y. Yue, S. Dolinar, M. Tur, and A. E. Willner, "Terabit free-space data transmission employing orbital angular momentum multiplexing," Nat. photonics, vol. 6, no. 7, pp. 488, 2012.

[8] R. Fickler, R. Lapkiewicz, W. N. Plick, M. Krenn, C. Schaeff, S. Ramelow, and A. Zeilinger, "Quantum entanglement of high angular momenta," Science, vol. 338, no. 6107, pp. 640-643, 2012.

[9] M. Padgett, and R. Bowman, "Tweezers with a twist," Nat. photonics, vol. 5, no. 6, pp. 343, 2011.

[10] N. M. Litchinitser, "Structured light meets structured matter," Science, vol. 337, no. 6098, pp. 1054-1055, 2012.

[11] F. Tamburini, G. Anzolin, G. Umbriaco, A. Bianchini, and C. Barbieri, "Overcoming the Rayleigh criterion limit with optical vortices," Phys. Rev. Lett., vol. 97, no. 16, pp. 3903, 2006.

[12] M. P. Lavery, F. C. Speirits, S. M. Barnett, and M. J. Padgett, "Detection of a spinning object using light's orbital angular momentum," Science, vol. 341, no. 6145, pp. 537-540, 2013.

[13] N. Zhang, X. C. Yuan, and R. E. Burge, "Extending the detection range of optical vortices by Dammann vortex gratings," Opt. Lett., vol. 35, no. 20, pp. 3495-3497, 2010.

[14] T. Lei, M. Zhang, Y. Li, P. Jia, G. N. Liu, X. Xu, Z. Li, C. Min, J. Lin, C. Yu, H. Niu and X. Yuan, "Massive individual orbital angular momentum channels for multiplexing enabled by Dammann gratings," Light Sci. Appl., vol. 4, no. 3, pp. e257, 2015.

[15] D. Deng, M. Lin, Y. Li and H. Zhao, "Precision Measurement of Fractional Orbital Angular Momentum," Phys. Rev. Appl., vol. 12, no. 1, pp. 014048, 2019.

[16] B. Guan, R. P. Scott, C. Qin, N. K. Fontaine, T. Su, C. Ferrari, M. Cappuzzo, F. Klemens, B. Keller, M. Earnshaw, and S. J. B. Yoo "Free-space coherent optical communication with orbital angular, momentum multiplexing/demultiplexing using a hybrid 3D photonic integrated circuit," Opt. Express, vol. 22, no. 1, pp. 145-156, 2014.

[17] X. Cai, J. Wang, M. J. Strain, B. Johnson-Morris, J. Zhu, M. Sorel, J. L. O'Brien, M. G. Thompson, S. Yu, "Integrated compact optical vortex beam emitters," Science, vol. 338, no. 6105, pp. 363-366, 2012.

[18] Z. Shao, J. Zhu, Y. Chen, Y. Zhang, and S. Yu, "Spin-orbit interaction of light induced by transverse spin angular momentum engineering," Nat. Commun., vol. 9, no. 1, pp. 926, 2018.

[19] Y. Li, X. Li, L. Chen, M. Pu, J. Jin, M. Hong, and X. Luo, "Orbital angular momentum multiplexing and demultiplexing by a single metasurface," Adv. Opt. Mater., vol. 5, no. 2, pp. 1600502, 2017.

[20] S. Zheng, and J. Wang, "Measuring orbital angular momentum (OAM) states of vortex beams with annular gratings," Sci. Rep., vol. **7**, pp. 40781, 2017.

[21] Z. Liu, S. Yan, H. Liu, and X. Chen, "Superhigh-Resolution Recognition of Optical Vortex Modes Assisted by a Deep-Learning Method," Phys. Rev. Lett., vol. 123, no. 18, pp. 3902, 2019.

[22] H. Zhou, S. Yan, J. Dong, and X. Zhang, "Double metal subwavelength slit arrays interference to measure the orbital angular momentum and the polarization of light," Opt. Lett., vol. 39, no. 11, pp. 3173-3176, 2014.

[23] D. Fu, D. Chen, R. Liu, Y. Wang, H. Gao, F. Li, and P. Zhang, "Probing the topological charge of a vortex beam with dynamic angular double slits," Opt. Lett., vol. 40, no. 5, pp. 788-791, 2015.

[24] N. K. Fontaine, R. Ryf, H. Chen, D. T. Neilson, K. Kim, and J. Carpenter, "Laguerre-Gaussian mode sorter," Nat. Commun., vol. 10, no. 1, pp. 1865, 2019.

[25] G. C. G. Berkhout, M. P. J. Lavery, J. Courtial, M. W. Beijersbergen, and M. J. Padgett, "Efficient sorting of orbital angular momentum states of light," Phys. Rev. Lett. vol. 105, no. 15, pp. 3601, 2010.

[26] B. Berger,M. Kahlert, D. Schmidt, and M. Assmann, "Spectroscopy of fractional orbital angular momentum states," Opt. Express, vol. 26, no. 32, pp. 248, 2018.

[27] J. Zhang, Y. Wen, H. Tan, J. Liu, L. Shen, M. Wang, J. Zhu, C. Guo, Y. Chen, Z. Li, and S. Yu, "80-Channel WDM-MDM Transmission over 50-km Ring-Core Fiber Using a Compact OAM DEMUX and Modular 4×4 MIMO Equalization," In Optical Fiber Communication Conference (Optical Society of America, 2019), pp. W3F-3.

[28] P. Gregg, P. Kristensen, and S. Ramachandran, "Conservation of orbital angular momentum in air-core optical fibers," Optica, vol. 2, no. 3, pp. 267-270, 2015.

[29] H. Xu, and L. Yang, "Conversion of orbital angular momentum of light in chiral fiber gratings," Opt. Lett., vol. 38, no. 11, pp. 1978-1980, 2013.

[30] X. Zhang, A. Wang, R. Chen, H. Ming and W. Zhao, "Generation of optical vortices by a pair of optical fiber orthogonal–dislocated gratings" J. Opt., vol. 21, no. 8, pp. 5707, 2019.

[31] M. V. Vasnetsov, V. A. Pas' Ko, and M. S. Soskin, "Analysis of orbital angular momentum of a misaligned optical beam," New J. Phys., vol. **7**, no. 1, pp. 46, 2005.

[32] G. Xie, H. Song, Z. Zhao, G. Milione, Y. Ren, C. Liu, R. Zhang, C. Bao, L. LI, Z. Wang, K. Pang, D. Starodubov, B. Lynn, M. Tur, and A. E. Willner "Using a complex optical orbital-angular-momentum spectrum to measure object parameters," Opt. Lett., vol. 42, no. 21, pp. 4482-4485, 2017.

[33] M. V. Berry, "Optical vortices evolving from helicoidal integer and fractional phase steps," J. Opt. A-pure Appl. Op., vol. 6, no. 2, pp. 259, 2004.

Guoxuan Zhu was born in Nanjing city, Jiangsu province, China in 1992. He received the B.S degree (2014), and Ph.D degree in optical enginnering (2019) from Sun Yat-sen University, Guangdong province, China. From 2018 to 2019, he was with the Optoelectronics Research Centre (ORC), University of Southampton, U.K., as a scholar visitor. Since 2019, he has been a Postdoctoral Researcher with the Guangdong and Hong Kong Joint Research Centre for Optical Fiber Sensors, Shenzhen University, Shenzhen, China. His current research interests include optical fiber, fiber communication, space-division multiplexing, fiber gratings, and optical orbital angular momentum.

Zhao Liu was born in Hebei, China, in 1996. He received the B.S. degree in Optoelectronic Information Science and Technology from Nanjing University of Posts and Telecommunications, in 2018. He currently focus on OAM mode control technology based on Few-Mode LPFG.

Cailing Fu was born in Hubei, China, in 1989. She received the M.S. degree in optical engineering from Wuhan Institute of Technology, Wuhan, China, in 2015 and the Ph.D degree in optical engineering from Shenzhen University, China, in 2018. From 2018 to 2020, she was with Shenzhen University, Shenzhen, China, as a Postdoctoral Research Fellow. Since 2020, she has been with Shenzhen University, Shenzhen, China, as an Assistant Professor. Her current research interests include optical fiber gratings and optical fiber sensors.

Shen Liu was born in Henan, China, in 1986. He received the B.Eng. degree in electronic and information engineering from PLA Air Force No.1 Aviation University, Changchun, China, in 2008, the M.S. degree in circuit and system from the Chongqing University of Posts and Telecommunications, Chongqing, China, in 2013, and the Ph.D. degree in optics from Shenzhen University, Shenzhen, China, in 2017. From 2017 to 2018, he was with Aston University, Birmingham, U.K., as a Postdoctoral Fellow. Since September 2018, he has been with Shenzhen University, as an Assistant Professor. His current research interests include optical fiber sensors, WGMs resonator, and cavity optomechanics. He has authored or coauthored 11 patent applications and more than 30 journal and conference papers.

Zhiyong Bai was born in Henan, China, in 1984. He received the B.S. degree in physics from Ningbo University, Ningbo, China, in 2008, the M.S. degree in optics from South China Normal University, Guangzhou, China, in 2011, and the Ph.D. degree in optics from Nankai University, Tianjin, China, in 2014. From 2014 to 2015, he has with the State Grid Electric Power Research Institute as an R&D Engineer. Since 2015, he has been a Postdoctoral Research Fellow with the Guangdong and Hong Kong Joint Research Centre for Optical Fiber Sensors, Shenzhen University, Shenzhen, China. His current research interests include optical fiber gratings, orbital angular momentum, and optical fiber sensors.

Yiping Wang (SM'11) was born in Chongqing, China, in 1971. He received the B.Eng. degree in precision instrument engineering from the Xi'an Institute of Technology, Xi'an, China, in 1995 and the M.S. and Ph.D. degrees in optical engineering from Chongqing University, Chongqing, China, in 2000 and 2003, respectively. From 2003 to 2005, he was with Shanghai Jiao Tong University, China, as a Postdoctoral Fellow. From 2005 to 2007, he was with the Hong Kong Polytechnic University, as a Postdoctoral Fellow. From 2007 to 2009, he was with the Institute of Photonic Technology (IPHT), Jena, Germany, as a Humboldt Research Fellow. From 2009 to 2011, he was with the Optoelectronics Research Centre (ORC), University of Southampton, U.K., as a Marie Curie Fellow. Since 2012, he has been with Shenzhen University, Shenzhen, China, as a Distinguished Professor. His current research interests include optical fiber sensors, fiber gratings, fiber miniature device and photonic crystal fibers. He has authored or coauthored one book, 21 patent applications, and more than 240 journal and conference papers. He is a Senior Member of the Optical Society of America and the Chinese Optical Society.